Triggering the Sintering of Silver Nanoparticles at Room Temperature

Shlomo Magdassi,[§,]* Michael Grouchko,[§] Oleg Berezin,[‡] and Alexander Kamyshny[§]

[§]Casali Institute for Applied Chemistry, Institute of Chemistry, The Hebrew University of Jerusalem, Jerusalem 91904, Israel, and [‡]MOBIChem Scientific Engineering Ltd., Jerusalem 91451, Israel

ABSTRACT A new approach to achieve coalescence and sintering of metallic nanoparticles at room temperature is presented. It was discovered that silver nanoparticles behave as soft particles when they come into contact with oppositely charged polyelectrolytes and undergo a spontaneous coalescence process, even without heating. Utilizing this finding in printing conductive patterns, which are composed of silver nanoparticles, enables achieving high conductivities even at room temperature. Due to the sintering of nanoparticles at room temperature, the formation of conductive patterns on plastic substrates and even on paper is made possible. The resulting high conductivity, 20% of that for bulk silver, enabled fabrication of various devices as demonstrated by inkjet printing of a plastic electroluminescent device.

KEYWORDS: silver nanoparticles · plastic electronics · coalescence · sintering

Metallic particles are considered hard materials, which are characterized by a high melting point (around 1000 °C) and large Young's modulus (~100 GPa). Therefore, coalescence and sintering of metallic particles are known to take place only under high pressure and high temperature[1−3] (for example, various metallic components are formed by sintering metal powders under pressure and high temperature).

Fabrication of electric circuits on heat-sensitive substrates such as paper, plastic packages, and polymeric substrates has attracted significant interest as a pathway to achieve flexible and low-cost electronic devices.[4−6] Inkjet is a nonimpact printing technology that can be utilized for direct printing of conductive patterns,[7] overcoming disadvantages of other printing methods such as lithography[8] and screen printing.[9]

The inkjet inks used for the fabrication of conductive patterns are aqueous or organic solvent dispersions of silver NPs that are stabilized by surfactants and polymers.[7,10,11] After printing and drying of the liquid, the resulting pattern is composed of conducting metallic NPs capped with organic stabilizers that act as an insulator. Due to the presence of this organic material between the particles, the number of percolation paths is limited, and the resistivity of the printed pattern is too high to be of practical importance. This obstacle is conventionally overcome by a sintering process, which is achieved by heating the printed substrates to temperatures usually higher than 200 °C in an oven[12−15] or by applying microwave[16] or laser[17,18] radiation. The sintering at 200 °C, which is much below the melting point of silver (960 °C), is usually attributed to the reduced melting point of NPs compared to that of bulk metal and to the surface premelting.[19−21] However, due to the sensitivity of most plastic substrates to high temperatures, such treatments are usually not suitable for these substrates, and therefore, fabrication of plastic flexible electronic devices is limited to a small number of heat-resistant polymers such as polyimide.

Here we report on a new approach to achieve sintering of metallic NPs at room temperature by a spontaneous three-dimensional (3D) coalescence process that takes place on solid substrates. The approach is based on triggering close packing of the NPs after being placed on a solid substrate, which eventually leads to their coalescence. The result is a sintered pattern that possesses high electrical conductivity. In the first part of this paper, we discuss the mechanism of the spontaneous 3D coalescence of silver NPs that are stabilized by poly(acrylic acid) (PAA), triggered by a cationic polymer, poly(diallyldimethylammonium chloride) (PDAC). In the second part, we show that this process enables achieving high electrical conductivity at room temperature and demonstrate how it can be utilized in an electroluminescence
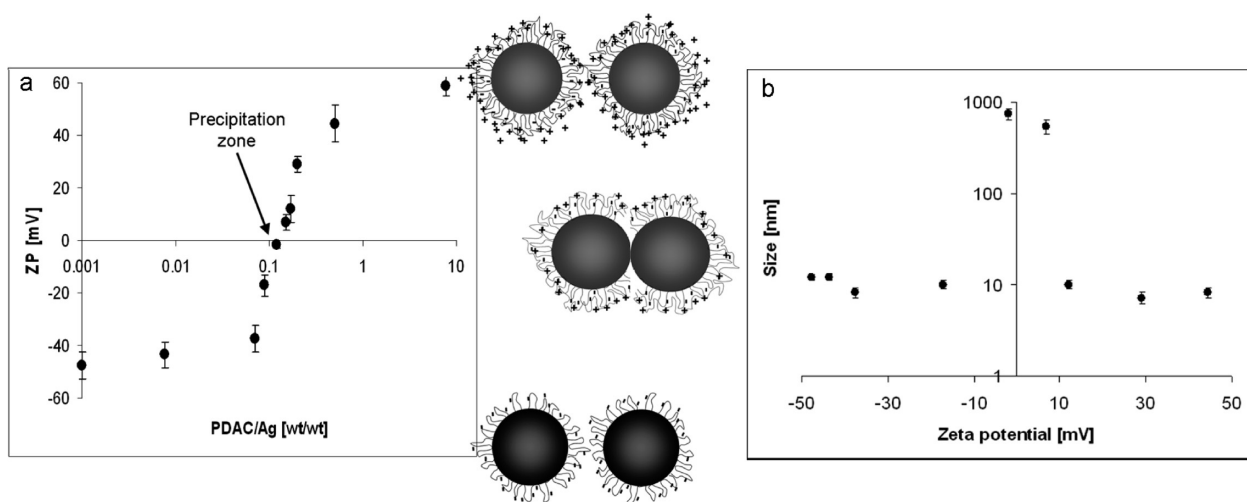
Figure 1. (a) Zeta-potential of silver NPs in aqueous dispersions and a schematic illustration of two states of silver NPs at various PDAC/Ag ratios; (b) particle size at various ζ-potential values. The silver NP concentration was set to 0.013 wt %, while the PDAC concentration varied from 0 to 0.1 wt %.

(EL) device on a poly(ethylene terephthalate) (PET) film.

RESULTS AND DISCUSSION

Coalescence of Metallic NPs at Room Temperature. At the first stage, we evaluated the ability of PDAC, a positively charged polymer, to cause aggregation in a dispersion of negatively charged silver NPs (5−80 nm in diameter, average diameter = 11.1 nm, 0.013 wt % metal content) that are stabilized by poly(acrylic acid) sodium salt (PAA). A series of PDAC solutions (0−0.1 wt %) were added to silver NP dispersions, and the zeta (ζ)-potential and average particle size were measured. The ζ-potential and average particle size of the dispersions (according to dynamic light scattering (DLS) measurements, Supporting Information Figure 4) as a function of PDAC concentration are presented in Figure 1. It can be seen that the ζ-potential of the original NPs is −47 ± 3 mV, and its negative value decreases with an increase in the PDAC concentration. At a PDAC/Ag (w/w) ratio of 0.12, the ζ-potential reaches a zero value, and precipitation of aggregated NPs occurs (average size ~700 nm, according to DLS). Characterization of the precipitated particles by HR-SEM (presented in the Supporting Information, Figure 1) clearly shows aggregates of the individual 10 nm silver NPs; that is, the aggregation was not followed by coalescence. As could be expected, higher PDAC/Ag ratio leads to positively charged silver nanoparticles. Schematic illustrations of the NPs before, at, and after the point of zero charge are also presented in Figure 1. As follows from the above data, at concentrations around the point of zero charge, PDAC acts as a coagulant for the metallic NPs by the charge neutralization mechanism.

At the next step, a similar experiment was performed but while the particles are present on a solid substrate. First, a film of concentrated (30 wt %) silver NP dispersion (wet thickness of 6 μm, by draw down)

was formed. After drying for 2 min at room temperature, an array of silver NPs with a thickness of about 0.5 μm was obtained. Then, a solution of polycations (PDAC, 1 wt %) was placed as droplets by inkjet printing on top of the silver array. Surprisingly, it was found that, within the zone of the printed droplets of the polycation, spontaneous sintering of all the silver NPs occurred without any heating. The difference between the sintered NPs within the polycation printed zone (Figure 2c) and the nonsintered NPs outside this zone (Figure 2a) is remarkable. As will be shown later, such coalescence leads to a significant increase in conductivity of the printed pattern.

In order to quantify the role of the polycation in the sintering process, drops of PDAC solutions at various concentrations were deposited on the top of a layer of silver NPs. HR-SEM images and the corresponding silver particle size distributions after coming into contact with drops having various concentrations of PDAC are presented in Figure 3. The size distribution was evaluated by image analysis; for nonspherical particles, the long axis of the particle was taken for the analysis. As shown, at a PDAC/Ag weight ratio lower than 0.01, the polycation does not affect the size and morphology of the particles (the size is similar to that found for the dispersion prior to coating it on the substrate). At higher PDAC/Ag weight ratios, the particle size increases as the PDAC concentration increases, and multiple percolation paths between particles are clearly observed. At PDAC/Ag weight ratio of 0.05, the average particle size increased significantly (larger than 120 nm), and at a ratio of 0.2, most of the particles are sintered, thus a continuous network of large particles is formed (it was impossible to perform size analysis of particles for this ratio). A cross-sectional SEM image of the sample at the PDAC/Ag ratio of 0.2 (Supporting Information, Figure 2) confirms that the coalescence process occurs throughout the whole thickness of the layer (~0.5 μm)
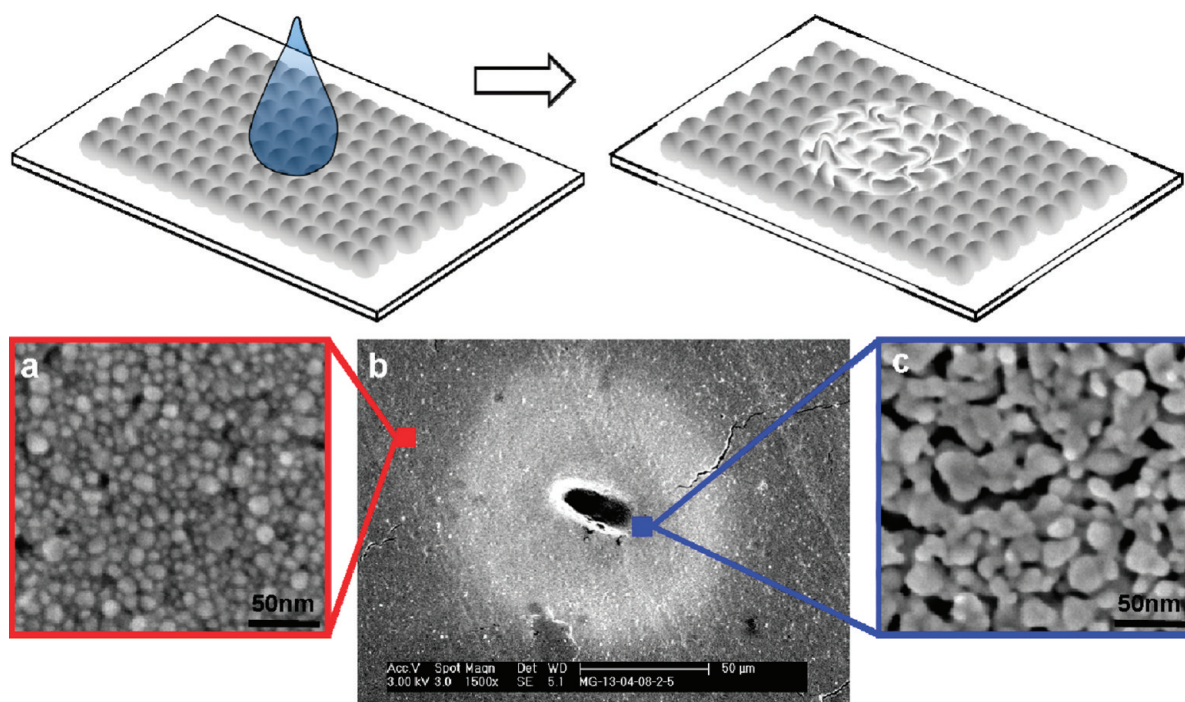
Figure 2. Top: Schematic illustration showing what happens when a droplet of PDAC solution is printed on silver NPs array. Bottom: SEM image of a printed drop zone (b) and the magnified images of NP arrays after the contact with PDAC outside (a) and inside (c) the droplet zone.

and not only on the surface; that is, the coalescence process takes place in three dimensions (it should be noted that the same morphology and structure were observed at higher PDAC/Ag weight ratios; results not shown).

As follows from the data presented in Figure 1, at PDAC concentrations around the point of zero charge, PDAC acts in the liquid dispersion as a coagulant for the silver NPs by a charge neutralization mechanism. Therefore, one could expect the same phenomenon will take place while adding the PDAC solution to NPs, which are deposited on a substrate; namely, the coagulation will take place only at the PDAC/Ag ratio at which charge neutralization occurs. However, the data presented in Figure 3 suggest that (a) the effect of PDAC on NPs that are predeposited onto a substrate is observed at a much lower PDAC/Ag ratio than in the liquid dispersion (0.01 and 0.1, respectively); (b) this effect is irreversible (*i.e.*, deaggregation was not observed), even at PDAC/Ag = 1; and (c) coalescence of the NPs
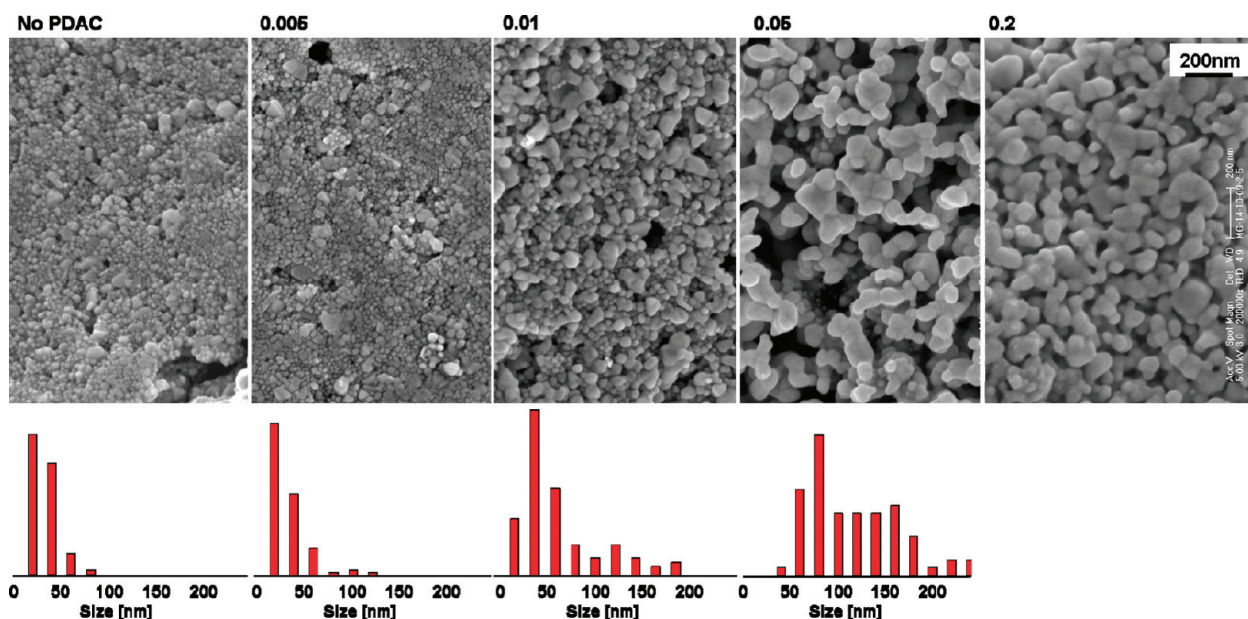

Figure 3. HR-SEM images and particle size distributions for printed patterns formed by silver NPs post-treated with PDAC at various PDAC/Ag ratios (the same magnification for all images).
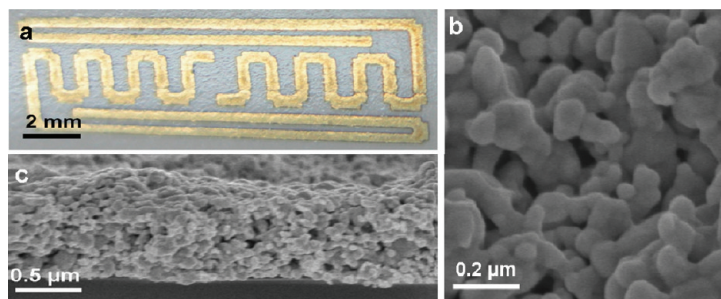
Figure 4. Macroscopic image of a pattern printed on Epson photo paper (a), HR-SEM images of the surface (b), and cross section (c) of the same pattern.

occurs while they are present on a solid substrate, while it does not happen in the liquid dispersion.

The difference in the observed effects of PDAC in a liquid dispersion and on a solid substrate may result from the restricted mobility of the particles on the substrate once they are closely packed. Upon coagulation, since the particles are already closely packed, contact between the metallic particles' surfaces may be formed, which leads to their coalescence. It should be noted that a possible mechanism that may also be involved is the desorption of the PAA from the NPs' surface due to electrostatic interaction with the PDAC,[22] leaving particles without their stabilizer and enabling their coalescence. Until now, such a coalescence of metallic nanoparticles was observed only under electron beam during HR-TEM characterization of individual NPs.[20,23−28] We showed that when two NPs are allowed to come close enough on a TEM grid the close contact is sufficient to trigger their coalescence.[29]

The sintering process that takes place at room temperature was also observed if the process was conducted *vice versa*; that is, drops of the silver dispersion were printed on top of a substrate that was precoated with a polycation solution. It was found that the resulting printed patterns of silver NPs on precoated glass and PET substrates were composed of sintered NPs (as clearly seen in the SEM images, Supporting Information Figure 3). Therefore, it can be concluded that the sintering at room temperature is not dependent on the chemical nature of the solid substrate.

Conductive Patterns and Application in Plastic Electronics. The applicability of this sintering process at room temperature for obtaining conductive patterns was evaluated on low-cost flexible paper and plastic substrates. The experiments were conducted by inkjet printing of silver NP dispersions on top of substrates containing a polycation. The substrates that were evaluated were (a) copier paper, (b) photo paper (Epson), and (c) a plastic (PET) EL device. The top layers of copier paper and the EL device were precoated by the polycation solution prior to printing the silver pattern. For the Epson photo paper, the precoating was not required because it already contains PDAC-like molecules (according to energy dispersive spectrometry (EDS) analysis, and in agreement with an Epson patent[30]). In general, it was

found that the particles within the patterns printed on the two types of papers were spontaneously sintered. In Figure 4, you can see the pattern printed on the photo paper (panel a), the SEM images of the sintered surface layer (panel b), and its cross-sectional area (panel c).

On the basis of these findings, it could be expected that the printed patterns composed of sintered NPs would be electrically conductive. Indeed, it was found that the printed patterns were conductive, having a sheet resistance and resistivity of 0.05 (±0.005) Ω/square and 6.8 (±0.5) μΩcm when printed on the Epson photo paper, and 0.68 (±0.07) Ω/square and 70 (±0.7) μΩcm when printed on the copier paper, respectively (these resistivities do not change for at least 6 months). It should also be emphasized that such low resistivities, only 5 times greater than the resistivity of bulk silver (in the case of the photo paper), have been reported until now only for silver patterns, which were sintered at elevated temperatures[12,15] for a prolonged time or post-treated by plasma[31] or high voltage,[32] while in the present study, it was achieved spontaneously at room temperature. It should be noted that in our system, although the sintering takes place in three dimensions, it leaves many voids between the sintered zones. This may indicate that the sintering stops at a certain range of particle' size. This hypothesis will be investigated in the future research.

The ability to decrease the resistivity of printed silver NPs was recently reported by Zapka et al.[33] They obtained the decrease of resistivity by contacting the printed pattern with 0.01 to 0.27 M NaCl solutions (by stamping), followed by heating to 95 °C. Low resistivities were obtained only at the highest NaCl concentration, which was a saturated solution. Although the mechanism of the sintering was not discussed, it is most likely that in that case the screening of surface charges due to increased ionic strength[34,35] has a significant role. In our case, the most probable mechanism involves the charge neutralization of the NPs or desorption of the stabilizer, which occurs at room temperature. Another possibility for sintering of NPs was recently reported by Wakuda et al.,[36] in which the printed pattern is dipped into a solvent, which probably leads to desorption of the particles stabilizer, dodecylamine. However, by that approach, very high resistivities were obtained.

In order to evaluate the applicability of this sintering technique for plastic electronics, a flexible, transparent PET-based EL device was constructed in two steps: (i) a four-layer (PET:ITO:ZnS:BaTiO₃) electroluminescence device (MOBIChem Scientific Engineering)[37] was coated by PDAC on the top of the BaTiO₃ layer and dried at room temperature; (ii) a silver dispersion was inkjet printed directly on the top of the PDAC layer (schematically illustrated in Figure 5). As seen in Figure

5, voltage (100 V) applied between the ITO and the silver electrodes resulted in light emission (90 cd/sqm) corresponding to the silver printed pattern. Thus, it can be concluded that, while the silver NPs are printed on top of the polycation coated substrate, the particles are sintered spontaneously and form an electrode.

In summary, a process for the coalescence of metallic NPs without heating was demonstrated. This process is triggered by modification of the surface properties of the NPs, by charge neutralization, and probably desorption of the stabilizer. At this stage, attempts to verify this hypothesis by performing surface analysis were not successful. The behavior of the metallic NPs as "soft particles" eventually resulted in sintering of the particles, without the required conventional heating process. As demonstrated for several solid substrates, porous and nonporous, the contact of the polycations with the oppositely charged NPs led to formation of a continuous 3D network, which enables electrical conductivity of the whole structure. On the basis of these findings, the sintering can be achieved either by placing a dispersion of metal NPs on a substrate precoated with the polyc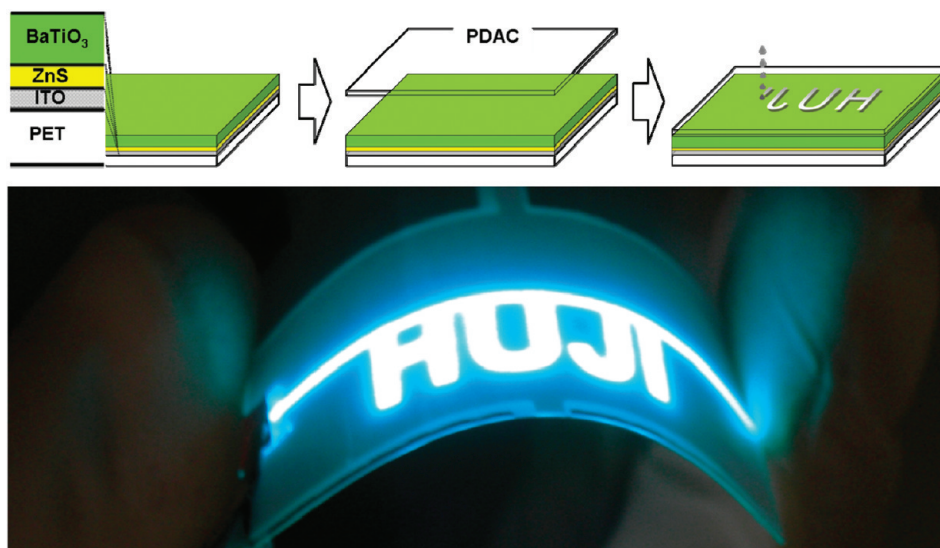ation, or *vice versa*, enabling conductive patterns on various temperature-sensitive substrates to be obtained. The use of this sintering process combined with inkjet printing to obtain highly conductive patterns was demonstrated on several substrates, including a plastic electroluminescent device. We expect that, by using this technology, the printing of conductive patterns on temperature-sensitive substrates would open new possibilities for applications in flexible and plastic electronics, including optoelectronic devices such as solar cells. The process can be conducted with coagulants other than polyelectrolytes and may be applied to other metals and other types of nanoparticles, such as quantum dots.

Figure 5. Top: Schematic illustration of the EL device and the printing process. Bottom: Electroluminescence working device.

EXPERIMENTAL SECTION

Silver NP Synthesis: Silver NPs with an average particle size of 10 nm were synthesized according to the following procedure: 4.5 g of silver acetate (Weiland) and 2.9 g of 20 wt % poly(acrylic acid) sodium salt (MW 8000, Aldrich) were mixed and heated to 95 °C for 15 min in 28 mL of triple distilled water (TDW). Then, 3.4 g of 30 wt % ascorbic acid was added, and the mixture was stirred for 30 min while heating. The obtained nanoparticles were washed by centrifugation, and the obtained sediment was redispersed in TDW. Then, the pH of the dispersion was adjusted to 9.5 by the addition of aminomethyl propanol (Acros); the silver concentration was set to 30 wt %, and the dispersion was sonicated for 10 min. The particle size distribution was measured by dynamic light scattering (DLS), and the results are presented in the Supporting Information (Figure 4). The dispersion was stable for at least 6 months at room temperature. This concentrated silver dispersion was used for the evaluation of the PDAC (MW = 450K) effect on the silver NPs on a substrate (Figures 2—5). In this experiment, a precise volume of PDAC (at various concentrations) was deposited on a silver pattern with a precise surface (so that the PDAC/Ag ratio can be calculated).

For the evaluation of the PDAC (MW = 450K) effect on the silver NPs in dispersion (Figure 1), the concentrated dispersion was diluted and the silver concentration was set to 0.013 wt %. The PDAC concentration in that experiment was in the range of 0 to 0.1 wt %.

Characterization Methods: HR-SEM images were obtained with Sirion (FEI) scanning electron microscope. Evaluation of the particle size by dynamic light scattering (DLS) and ζ-potential analyses were performed using a Zetasizer nano-SZ (Malvern Instruments).

PDAC Treatment: The pretreatment of substrates (glass, PET, and paper) by PDAC was carried out by a draw down method, with a 6 μm wet thickness of 0.1 wt % PDAC solution. In the case of the electroluminescence device, a wetting agent (0.1 wt % BYK 348) was added to the PDAC solution in order to obtain a homogeneous layer. The post-treatment of silver patterns by PDAC was carried out by depositing 50 μL of PDAC solution (0.001 to 20 wt %) on top of the 26 $\times$ 76 mm silver patterns.

Inkjet Printing: The PDAC solution (Figure 2) was printed with the use of a JetDrive III controller (MicroFab) with a 60 μm orifice print head. The silver ink was printed with a commercial Lexmark Z615 office printer.

Resistivity Measurements: The resistivity of printed patterns was calculated by measuring the printed line resistance by a milliohm meter (EXTECH) and measuring the thickness profile by HR-SEM. The sheet resistances were measured by a four point probe (Cascade Microtech Inc.).

REFERENCES AND NOTES

1. Frenkel, J. Viscous Flow of Crystaline Bodies under the Action of Surface Tension. *J. Phys. (Paris)* **1945**, *9*, 385–391.

2. Gutmanas, E. Y.; Rabinkin, A.; Roitberg, M. Cold Sintering under High-Pressure. *Scr. Mater.* **1979**, *13*, 11–15.

3. Kraft, T.; Riedel, H. Numerical Simulation of Solid State Sintering; Model and Application. *J. Eur. Ceram. Soc.* **2004**, *24*, 345–361.

4. Garnier, F.; Hajlaoui, R.; Yassar, A.; Srivastava, P. All-Polymer Field-Effect Transistor Realized by Printing Techniques. *Science* **1994**, *265*, 1684–1686.

5. Eda, G.; Fanchini, G.; Chhowalla, M. Large-Area Ultrathin Films of Reduced Graphene Oxide as a Transparent and Flexible Electronic Material. *Nat. Nanotechnol.* **2008**, *3*, 270–274.

6. Forrest, S. R. The Path to Ubiquitous and Low-Cost Organic Electronic Appliances on Plastic. *Nature* **2004**, *428*, 911–918.

7. van Osch, T. H. J.; Perelaer, J.; de Laat, A. W. M.; Schubert, U. S. Inkjet Printing of Narrow Conductive Tracks on Untreated Polymeric Substrates. *Adv. Mater.* **2008**, *20*, 343–345.

8. Park, I.; Ko, S. H.; Pan, H.; Grigoropoulos, C. P.; Pisano, A. P.; Frechet, J. M. J.; Lee, E. S.; Jeong, J. H. Nanoscale Patterning and Electronics on Flexible Substrate by Direct Nanoimprinting of Metallic Nanoparticles. *Adv. Mater.* **2008**, *20*, 489–496.

9. Merilampi, S.; Laine-Ma, T.; Ruuskanen, P. The Characterization of Electrically Conductive Silver Ink Patterns on Flexible Substrates. *Microelectron. Reliab.* **2009**, *49*, 782–790.

10. Sivaramakrishnan, S.; Chia, P. J.; Yeo, Y. C.; Chua, L. L.; Ho, P. K. H. Controlled Insulator-to-Metal Transformation in Printable Polymer Composites with Nanometal Clusters. *Nat. Mater.* **2007**, *6*, 149–155.

11. Kim, D.; Jeong, S.; Park, B. K.; Moon, J. Direct Writing of Silver Conductive Patterns: Improvement of Film Morphology and Conductance by Controlling Solvent Compositions. *Appl. Phys. Lett.* **2006**, *89*, 264101.

12. Fuller, S. B.; Wilhelm, E. J.; Jacobson, J. A. Ink-Jet Printed Nanoparticle Microelectromechanical Systems. *J. Microelectromech. Syst.* **2002**, *11*, 54–60.

13. Joo, S.; Baldwin, D. F. Performance of Silver Nano Particles as an Electronics Packaging Interconnects Material. *Elec. Comp. C* **2007**, 212–226.

14. Szczech, J. B.; Megaridis, C. M.; Zhang, J.; Gamota, D. R. Ink Jet Processing of Metallic Nanoparticle Suspensions for Electronic Circuitry Fabrication. *Microscale Therm. Eng.* **2004**, *8*, 327–339.

15. Kim, D.; Moon, J. Highly Conductive Ink Jet Printed Films of Nanosilver Particles for Printable Electronics. *Electrochem. Solid State* **2005**, *8*, J30–J33.

16. Perelaer, J.; de Gans, B. J.; Schubert, U. S. Ink-Jet Printing and Microwave Sintering of Conductive Silver Tracks. *Adv. Mater.* **2006**, *18*, 2101–2104.

17. Ko, S. H.; Pan, H.; Grigoropoulos, C. P.; Luscombe, C. K.; Frechet, J. M. J.; Poulikakos, D. Air Stable High Resolution Organic Transistors by Selective Laser Sintering of Ink-Jet Printed Metal Nanoparticles. *Appl. Phys. Lett.* **2007**, *90*, 141103.

18. Bieri, N. R.; Chung, J.; Poulikakos, D.; Grigoropoulos, C. P. Manufacturing of Nanoscale Thickness Gold Lines by Laser Curing of a Discretely Deposited Nanoparticle Suspension. *Superlattice Microstruct.* **2004**, *35*, 437–444.

19. Frenken, J. W. M.; Vanderveen, J. F. Observation of Surface Melting. *Phys. Rev. Lett.* **1985**, *54*, 134–137.

20. Lewis, L. J.; Jensen, P.; Barrat, J. L. Melting, Freezing, and Coalescence of Gold Nanoclusters. *Phys. Rev. B* **1997**, *56*, 2248–2257.

21. Moon, K. S.; Dong, H.; Maric, R.; Pothukuchi, S.; Hunt, A.; Li, Y.; Wong, C. P. Thermal Behavior of Silver Nanoparticles for Low-Temperature Interconnect Applications. *J. Electron. Mater.* **2005**, *34*, 168–175.

22. Rojas, O. J.; Ernstsson, M.; Neuman, R. D.; Claesson, P. M. Effect of Polyelectrolyte Charge Density on the Adsorption and Desorption Behavior on Mica. *Langmuir* **2002**, *18*, 1604–1612.

23. Buffat, P. A. Electron Diffraction and HRTEM Studies of Multiply-Twinned Structures and Dynamical Events in Metal Nanoparticles: Facts and Artefacts. *Mater. Chem. Phys.* **2003**, *81*, 368–375.

24. Palasantzas, G.; Vystavel, T.; Koch, S. A.; De Hosson, J. T. M. Coalescence Aspects of Cobalt Nanoparticles during *In Situ* High-Temperature Annealing. *J. Appl. Phys.* **2006**, *99*, 024307.

25. Jose-Yacaman, M.; Gutierrez-Wing, C.; Miki, M.; Yang, D. Q.; Piyakis, K. N.; Sacher, E. Surface Diffusion and Coalescence of Mobile Metal Nanoparticles. *J. Phys. Chem. B* **2005**, *109*, 9703–9711.

26. Hawa, T.; Zachariah, M. R. Coalescence Kinetics of Unequal Sized Nanoparticles. *J. Aerosol. Sci.* **2006**, *37*, 1–15.

27. Chen, Y.; Palmer, R. E.; Wilcoxon, J. P. Sintering of Passivated Gold Nanoparticles under the Electron Beam. *Langmuir* **2006**, *22*, 2851–2855.

28. Buffat, P. A. Dynamical Behaviour of Nanocrystals in Transmission Electron Microscopy: Size, Temperature or Irradiation Effects. *Philos. Trans. R Soc., A* **2003**, *361*, 291–295.

29. Grouchko, M.; Popov, I.; Uvarov, V.; Magdassi, S.; Kamyshny, A. Coalescence of Silver Nanoparticles at Room Temperature: Unusual Crystal Structure Transformation and Dendrite Formation Induced by Self-Assembly. *Langmuir* **2009**, *25*, 2501–2503.

30. Hanmura, M.; Onishi, H.; Kubota, N.; Asai, S.; Yoshizawa, S.; Tatsuhashi, F.; Katagiri, K.; Tsushida, M.; Iwamoto, K. Jpn Patent JP2002211115 (A), 2002.

31. Reinhold, I.; Hendriks, C. E.; Eckardt, R.; Kranenburg, J. M.; Perelaer, J.; Baumann, R. R.; Schubert, U. S. Argon Plasma Sintering of Inkjet Printed Silver Tracks on Polymer Substrates. *J. Mater. Chem.* **2009**, *19*, 3384–3388.

32. Allen, M. L.; Aronniemi, M.; Mattila, T.; Alastalo, A.; Ojanpera, K.; Suhonen, M.; Seppa, H. Electrical Sintering of Nanoaparticles Structures. *Nanotechnology* **2008**, *19*, 175201–175204.

33. Zapka, W.; Voit, W.; Loderer, C.; Lang, P. Low Temperature Chemical Post-Treatment of Inkjet Printed Nano-Particle Silver Inks. *Digital Fabrication 2008*; 2008; pp 906–911.

34. Tadros, T. F. *Colloid Stability*; Wiley-VCH: Weinheim, Germany, 2007.

35. Everett, D. H. *Basic Principles of Colloid Science*; The Royal Society of Chemistry: Letchworth, UK, 1988.

36. Wakuda, D.; Kim, K.; Suganuma, K. Room-temperature Sintering of Ag Nanoaprticles Paste. *IEEE Trans. Compon., Packag. Technol.* **2009**, *32*, 627–632.

37. Yoshida, M.; Mikami, A.; Inoguchi, T.; Miura, N. *Phosphor Handbook*; CRC Press: Boca Raton, FL, 2006.